Dynamic Scaling and Island Growth Kinetics in Pulsed Laser Deposition of $SrTiO_3$

Gyula Eres,[1,*] J. Z. Tischler,[2] C. M. Rouleau,[3] Ho Nyung Lee,[1] H. M. Christen,[3] P. Zschack,[2,4] and B. C. Larson[1]
[1]*Materials Science and Technology Division, Oak Ridge National Laboratory, Oak Ridge, Tennessee 37831, USA*
[2]*X-Ray Science Division, Advanced Photon Source, Argonne National Laboratory, Argonne, Illinois 61801, USA*
[3]*Center for Nanophase Materials Sciences, Oak Ridge National Laboratory, Oak Ridge, Tennessee 37831, USA*
[4]*Photon Sciences Division, Brookhaven National Laboratory, Upton, New York 11973, USA*
(Received 13 April 2016; revised manuscript received 12 August 2016; published 11 November 2016)

We use real-time diffuse surface x-ray diffraction to probe the evolution of island size distributions and its effects on surface smoothing in pulsed laser deposition (PLD) of $SrTiO_3$. We show that the island size evolution obeys dynamic scaling and two distinct regimes of island growth kinetics. Our data show that PLD film growth can persist without roughening despite thermally driven Ostwald ripening, the main mechanism for surface smoothing, being shut down. The absence of roughening is concomitant with decreasing island density, contradicting the prevailing view that increasing island density is the key to surface smoothing in PLD. We also report a previously unobserved crossover from diffusion-limited to attachment-limited island growth that reveals the influence of nonequilibrium atomic level surface transport processes on the growth modes in PLD. We show by direct measurements that attachment-limited island growth is the dominant process in PLD that creates step flowlike behavior or quasistep flow as PLD "self-organizes" local step flow on a length scale consistent with the substrate temperature and PLD parameters.

DOI: 10.1103/PhysRevLett.117.206102

Interface sharpness is a critical thin film variable that regulates the interplay between the lattice, charge, orbital, and spin degrees of freedom in exploring novel condensed matter physics phenomena using complex oxide heterostructures [1]. Recent advances in pulsed laser deposition (PLD) have enabled the growth of a wide range of complex oxide superlattices with atomically sharp interfaces. However, the fundamental mechanism leading to atomically sharp interface formation in PLD, also referred to as "surface smoothing," remains highly controversial [2–4].

The ideal mode for growing atomically sharp interfaces is step flow that produces a perfect replica of the initial surface [5]. Step flow involves the simplest form of atomic surface transport—horizontal (intralayer) transport, also known as surface diffusion–of the growth species. However, if the diffusion length becomes smaller than the terrace width, step flow breaks down [6] by random nucleation leading to island growth on terraces that changes the growth mode to layer-by-layer (LBL) growth. Achieving atomically sharp interfaces in LBL growth requires an additional surface transport mechanism for promoting vertical (interlayer) transport of the growth species [7–9]. The ability to uncouple surface transport processes from substrate heating and enhancing interlayer transport independently makes PLD distinctly different from thermal deposition (TD) processes such as MBE [10]. These nonthermal processes dramatically expand the film growth parameter space compared to TD [2,10] making PLD an important method for exploring energy enhanced film growth physics [11,12].

Central to understanding the mechanism of surface smoothing for either PLD or TD is the concept of critical island size for LBL growth [13]. Smooth LBL growth requires that the critical island size remain larger than the average island spacing; otherwise, multilayer growth and eventually three-dimensional (3D) surface roughening set in. The prevailing view is that the beneficial effects of PLD derive primarily from the very high supersaturation, which according to classical nucleation theory produces very high island densities [11] and reduced island spacing. Because island coalescence leads to exceeding the critical island size, it also marks the onset of second layer nucleation. It is postulated that the superthermal kinetic energy in PLD is channeled into the nonthermal surface mobility necessary to achieve full coverage by filling the remaining holes past coalescence [14–17]. For instance, modeling surface transport for the deposition of Pt showed that hyperthermal kinetic energy atoms enhance both intra- and interlayer transport [12]. Because kinetic energy effects are difficult to probe directly, island density measurements are typically used in searching for defining features that differentiate PLD from TD methods [10,11]. Accordingly, there have been a number of both experimental and theoretical reports comparing the island densities between PLD and TD [10,11,18].

The understanding of PLD film growth mechanisms has been greatly advanced by recent results obtained by surface x-ray diffraction (SXRD) [3,4,9,14,15]. However, these experiments still do not capture the complete PLD growth mechanism. The specular intensity that is measured in most experiments describes only the distribution of atoms in layers along increasing thickness (surface normal), but provides no information about how the atoms are distributed in each particular layer. Here, we discuss the missing component of the PLD growth kinetics concerning the distribution of atoms in the horizontal direction that is contained in the evolution of island size distributions (ISDs). We performed real-time measurements of the diffuse scattering from which we extract a length scale describing the ISD for individual laser shots during the PLD growth of $SrTiO_3$. The data reveal that island size evolution obeys dynamic scaling with two distinct kinetic regimes and that PLD "self-organizes" local step flow on a length scale governed by the temperature and the PLD growth conditions. We demonstrate that quasistep flow becomes dominant as the correlation length increases (island density decreases) with ordinary step flow being its asymptotic limit [5].

The scattered SXRD intensity signal in general consists of the following three components $I(q) = I_{\mathrm{coh}}(q=0) + I_{\mathrm{diff}}(q \neq 0) + I_{\mathrm{bak}}$ where $I_{\mathrm{coh}}(q=0)$ represents the specular component, $I_{\mathrm{diff}}(q \neq 0)$ is the diffuse scattering, and I_{bak} is a small background component that is negligible in these experiments. The details of the experimental measurements are provided in Supplemental Material [19]. The 3D line plot in Fig. 1 shows that the diffuse scattering in the bottom plane and the specular intensity in the back plane oscillate $\pi/2$ out of phase. The position of the diffuse side lobes and the intensity distribution in the diffuse scattering peak are the SXRD representation of the ISD function $f(r,t) \propto I_{\mathrm{diff}}(q \neq 0, t)$ for each laser shot. By restricting the analysis to diffraction profiles obtained only near half layer $\theta \approx 0.5$ coverages, the island separation function has a negligible contribution from incomplete multiple levels. In agreement with the simultaneous two layer growth described in previous reports [9,15] the surface morphology is dominated by isolated islands, and it is sufficient to show that the functional form remains unchanged under different growth conditions. The confirmation of dynamic scaling indicative of a conserved ISD is illustrated in Fig. 2. It implies that island size evolution is characterized by a single length scale [22], which can be extracted directly from the experimental data as the separation Δq between the maximum of the diffuse peak and the position of the specular peak. Δq is in turn related to the correlation length $\ell = (2\pi/\Delta q)$ that is governed by the distributions of both the island spacings and the island sizes.

The key feature of the diffuse scattering data in Fig. 1 is that Δq decreases with successive laser shots. Considering that ℓ provides a measure of the island spacing, a decreasing Δq corresponds to increasing island size and a concomitant decrease in island density. From the relationship between Δq and ℓ, the island density $N(t)$ is given by $N(t) \sim (\Delta q)^2$. In the absence of coalescence of mobile islands the island density in the precoalescence stage can be assumed to be roughly equal to the nucleation density. In the virgin surface submonolayer regime the increase in ℓ with successive laser shots is straightforward to understand in terms of (1) increasing coverage, (2) island coarsening by ripening, and (3) the reduction of the number of islands by coalescence past half coverage. If this cycle were to repeat itself for each new layer, and the next layer were to start growing at the same nucleation density, Δq would recover its initial value. However, the continuously decreasing initial Δq values indicate that the new layers do not renucleate by the same mechanism as the first layer. Rather,

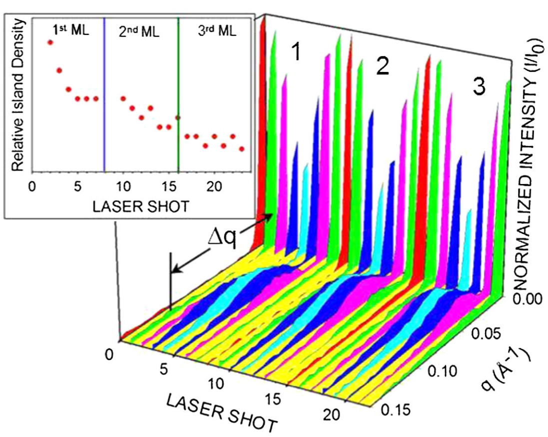

FIG. 1. 3D line plot of the SXRD intensities as a function of q for single laser shots of $SrTiO_3$ growth at 650 °C and a 10 s dwell time that corresponds to the time between successive laser shots. The growth intensity oscillations for the growth of the first three MLs are shown on the back (vertical) plane, and the out of phase diffuse scattering oscillations are shown on the front (horizontal) plane. A ML corresponds to a unit cell consisting of one SrO/TiO_2 bilayer. The inset shows the corresponding island densities extracted from the diffuse scattering data as $N(t) \sim (\Delta q)^2$ for the first three unit cell growth.

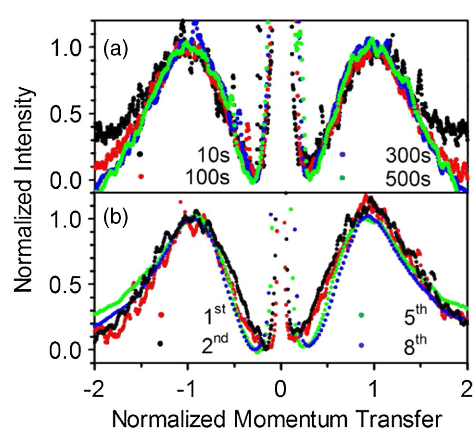

FIG. 2. Demonstration of the scaling of ISD after background subtraction and normalization of both the horizontal and the vertical axes. (a) Scaling for diffusion-limited $n = \frac{1}{3}$ island growth measured at 10, 100, 300, and 500 s after deposition of $\theta = 0.5$ and annealing at 700 °C. The data are shown in Fig. S2(a) [19]. (b) Scaling for attachment-limited $n = \frac{1}{2}$ island growth determined for the diffuse scattering maxima after growing one, two, five, and eight MLs of $SrTiO_3$ at a fixed substrate temperature of 700 °C and a 10 s dwell time. The data are shown in Fig. S1(c) [19].

the observation of decreasing Δq for subsequent growth indicates that island nucleation in each new layer occurs with a larger length scale than the previous layer. Thus, the measurements reveal a nucleation behavior that is not consistent with supersaturated nucleation density dominated film growth models.

To be specific, the decreasing island density for single laser shots in the growth of the first three MLs is illustrated in the inset of Fig. 1. The correlation length is smallest (corresponding to the highest island density) in the first layer with the growth of each successive layer occurring at a decreasing island density. Moreover, we note that in no case was Δq observed to increase with increasing deposition pulses, ruling out the island breakup mechanism proposed for increasing the island density [3]. Instead, as underscored by the additional data presented in the Supplemental Material [19], the diffuse scattering measurements demonstrate that decreasing island densities are a universal feature of PLD that occurs over a wide range of dwell times and temperatures.

Turning now to island growth kinetics, theoretical treatments show that the mechanism of the attachment-detachment process dictates the functional form of the ISD [23,24]. The temporal power law dependence $\ell(t) \propto t^n$ is used for describing the evolution of the mean island size [as measured by the critical length scale $\ell(t)$]. The value of the exponent n determines the island growth mechanism that is governed by atomistic barriers and surface transport processes in island nucleation, growth, and ripening [25–27]. We show in Fig. 3 plots of the correlation length versus time derived from the x-ray intensity maps, where the series of points given by the different symbols represent the correlation length $\ell = (2\pi/\Delta q)$ at the diffuse scattering maxima increasing in ML increments.

These plots reveal that island growth in PLD does not obey the simple kinetics described by a single value of n. Rather, two distinctly different slopes in which the short (first) segments denoted by dashed lines are shown to extend with a slope close to $n = \frac{1}{3}$ to the third ML (at most), thus indicating island coarsening controlled by diffusion limited kinetics. The major (longer) segments describe the kinetics for the bulk of the island growth and evolution process. For all films the major segment has a value of n equal to or greater than $n = \frac{1}{2}$, suggesting attachment-detachment limited kinetics. The crossover from diffusion-limited to attachment-detachment kinetics [27] that occurs over a limited island size range at each temperature is attributed to the island edges becoming energetically more stable with increasing size that decreases curvature.

Having identified two kinetic regimes we show in Fig. S2(a) [19] measurements probing specifically the diffusion-limited regime by using a single laser shot to deposit a layer coverage $\theta \approx 0.5$ on a virgin surface, followed by extended annealing at a fixed substrate temperature. These conditions preclude second layer nucleation, thus rendering interlayer transport nonexistent. The postdeposition evolution of the ISD represents a textbook example of the Ostwald ripening of 2D islands. The correlation lengths were determined by measuring the diffuse scattering at 10 s intervals. The evolution of $\ell(t)$ plotted in Fig. 3 by the black circles after a short transition section has a slope of $n = 0.35$. This value is in agreement with the $n = \frac{1}{3}$ expectation that ripening dominated by intralayer transport is controlled by diffusion-limited kinetics. On the basis of having the same slope as in the single shot $\theta \approx 0.5$ annealing experiment, we can conclude that coarsening in the first few layers during the minor or short stage of simultaneous two-layer growth is also driven by surface diffusion. We note that this value is in agreement with a report [4] that used measurements of the diffuse scattering to conclude (based only on first ML data) that surface smoothing in PLD occurs by thermal ripening. However, no analysis of the kinetics in subsequent layers was performed in that study, so the change in the island growth regime was not observed [4].

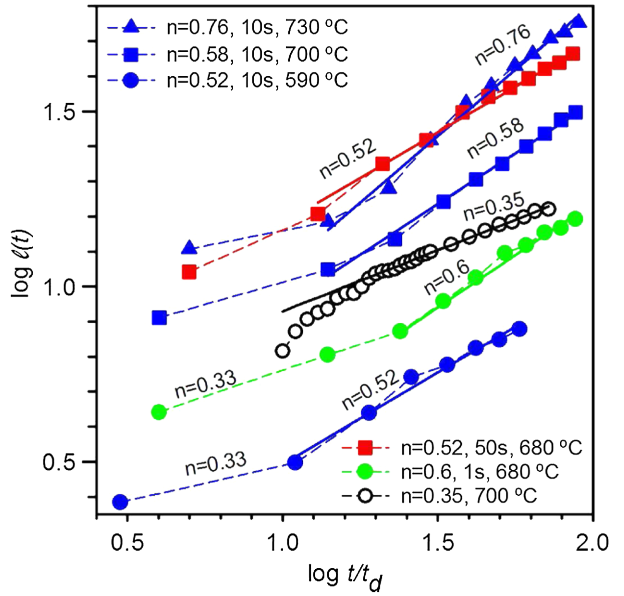

FIG. 3. Evolution of island growth during PLD represented by a log-log plot of $\ell(t)$ vs t/t_d, where t_d represents a time interval that for growth corresponds to the dwell time between two successive laser shots, and for annealing to the measurement time steps. The different colors represent different dwell times, and the different shape blue symbols designate different substrate temperatures for the data in Fig. S1 [19]. The black circles represent the thermal coarsening data in Fig. S2(a) [19], corresponding to an infinite effective dwell time. The value of n on the dashed and solid lines corresponds to the exponent of the power law fit.

The absence of thermal ripening between two successive laser shots is a new observation that provides important clues for understanding the role of atomic surface transport processes in the mechanism of PLD film growth. To pursue this aspect, an experiment was performed in which growth was stopped at the diffuse scattering maximum after $2\frac{1}{2}$ MLs and the diffracted intensity was measured continuously at 10 s intervals. Note also that this thickness was chosen deliberately to ensure that the kinetics is measured just past the $\frac{1}{3}$ to $\frac{1}{2}$ crossover point. An analysis of the data plotted in Fig. 4 shows that $\ell(t)$ given by red triangles remains unchanged even 300 s after the deposition was stopped, indicating negligible ripening and no change in the ISD at 640 °C. These data are to be compared with measurements on a second film that was grown under exactly the same conditions, but without the interruption of growth. The blue dots show that the two data sets overlap for the first $\sim 2\frac{1}{2}$ MLs, but past this thickness, $\ell(t)$ continues to increase with a slope of $n = 0.53$, if growth is continued. The most significant implication of a frozen $\ell(t)$ is that it rules out Ostwald ripening, which is the primary mechanism for surface smoothening in TD. On the atomic level this implies that the barrier for detachment from step edges is so high that it prevents the thermally driven transfer of atoms from smaller to larger islands. With detachment frozen, negligible thermal ripening implies that surface smoothing must be driven solely by the attachment-limited nonequilibrium island growth that occurs only in the presence of continued deposition pulses. Although the driving forces are different, the outcome is equivalent to step flow on the scale of the island sizes.

The complete data covering a wide range of growth conditions in Fig. S1 [19] that were used for deriving the island size evolution plots in Fig. 3 also illustrate a remarkable feature of PLD; that is, simultaneous two layer growth persists indefinitely in a quasistep flow mode with increasing island sizes, and without observable surface roughening. Accordingly, island growth from the laser pulse must be faster than the time scale of the fastest diffuse scattering measurements, which at a 1 s dwell time still show attachment-limited kinetics. Moreover, since ripening does not occur during the dwell time, the

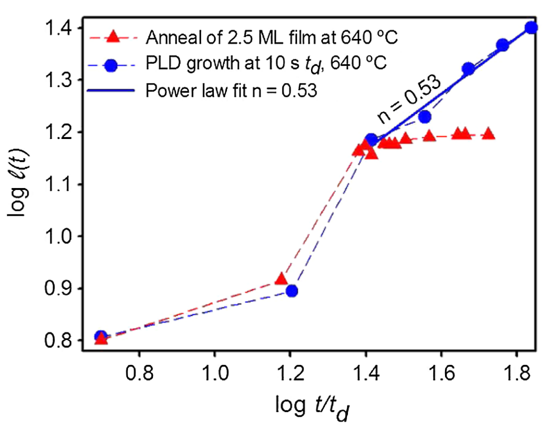

FIG. 4. Illustration of the negligible change of the correlation length (red triangles) for a $SrTiO_3$ film that was annealed at a substrate temperature of 640 °C after growth was stopped at the third diffuse scattering maximum ($\sim 2\frac{1}{2}$ ML) compared to the increasing correlation length in continuous film growth (blue dots). The complete data are shown in Fig. S2(b) [19].

crystallization time represents the best estimate for the duration of island growth in PLD. We reported this previously to be faster than a few microseconds [15].

Theoretical simulations show that the increase in n from $\frac{1}{3}$ for purely diffusion-limited kinetics, to $\frac{1}{2}$ for attachment-limited kinetics [27], is driven by fundamental changes in atomic surface transport processes. The expanded discussion of the connection to atomic surface transport processes presented in the Supplemental Material [19] shows that the ratio D/k fully captures the unique features of PLD growth for a crossover from diffusion-limited ($(D/k) \ll 1$) to attachment-limited ($(D/k) \gg 1$) growth, where D is the surface diffusivity, and k is the attachment rate. The half coverage annealing results in Fig. 3 and Fig. S2(a) [19] show that thermally driven attachment and detachment must be present in the diffusion-limited $n = \frac{1}{3}$ regime. Consequently, this cannot be the mechanism of PLD growth past two MLs; it is just thermally driven, ordinary Ostwald ripening. The frozen detachment past $\sim 2\frac{1}{2}$ in Fig. 4 implies that the island growth occurs by direct incorporation of growth species from the PLD plume. In addition, for attachment to change the ratio to $(D/k) \gg 1$, and become rate limiting, the growth species must possess ballistic mobilities [16,17] capable of inducing very fast intra- and interlayer transport [9,15]. This ballistic component is of course always present in PLD island growth. Here, we show that when detachment is frozen the effects of ballistic mobility can be observed directly. In the absence of Ehrlich-Schwoebel and other island edge barriers [28], it can be assumed that the attachment rate k is constant in both the diffusion-limited and the attachment-limited regimes, leading to the conclusion that the crossover occurs when the surface mobilities D change from thermal diffusion (that is much slower than attachment) to ballistic mobility in the PLD plume [15–17] that is much faster than attachment. This evolves spontaneously at a given temperature as the increasing size reduces island curvature causing the islands to energetically stabilize against detachment.

In summary, we address the mechanisms of island growth leading to surface smoothing in PLD through real-time measurements of the diffuse scattering. We demonstrate that island size evolution during PLD of $SrTiO_3$ obeys dynamic scaling, which allows the identification of two distinct regimes of island growth kinetics. The decreasing island density and a crossover from diffusion-limited to attachment-limited kinetics rule out increasing nucleation density as a factor in surface smoothing. The crossover identifies a fundamental change in the surface transport mechanisms, and reveals the influence of nonequilibrium and nonthermal atomic level surface transport processes on the growth modes in PLD. Our measurements show that in this regime PLD film growth persists without surface roughening, despite Ostwald ripening, the main thermally driven smothening mechanism being shut down. In this quasistep flow regime PLD self-organizes local step flow on a length scale consistent with the temperature and PLD conditions. It is an intriguing question whether the crossover in island growth kinetics that was discussed theoretically [27], but not previously observed experimentally, is unique to PLD mechanisms.

This research was sponsored by the U.S. Department of Energy (DOE), Office of Science, Basic Energy Sciences, Materials Sciences and Engineering Division. This research used resources of the Advanced Photon Source, a U.S. Department of Energy (DOE) Office of Science User Facility operated for the DOE Office of Science by Argonne National Laboratory under Contract No. DE-AC02-06CH11357.

*eresg@ornl.gov

[1] H. Y. Hwang, Y. Iwasa, M. Kawasaki, B. Keimer, N. Nagaosa, and Y. Tokura, Nat. Mater. **11**, 103 (2012).
[2] H. M. Christen and G. Eres, J. Phys. Condens. Matter **20**, 264005 (2008).
[3] P. R. Willmott, R. Herger, C. M. Schleputz, D. Martoccia, and B. D. Patterson, Phys. Rev. Lett. **96**, 176102 (2006).
[4] J. D. Ferguson, G. Arikan, D. S. Dale, A. R. Woll, and J. D. Brock, Phys. Rev. Lett. **103**, 256103 (2009).
[5] H.-C. Jeong and E. D. Williams, Surf. Sci. Rep. **34**, 171 (1999).
[6] W. Hong, H. N. Lee, M. Yoon, H. M. Christen, D. H. Lowndes, Z. Suo, and Z. Zhang, Phys. Rev. Lett. **95**, 095501 (2005).
[7] K. Bromann, H. Brune, H. Roder, and K. Kern, Phys. Rev. Lett. **75**, 677 (1995).
[8] Z. Zhang and M. G. Lagally, Science **276**, 377 (1997).
[9] G. Eres, J. Z. Tischler, C. M. Rouleau, P. Zschack, H. M. Christen, and B. C. Larson, Phys. Rev. B **84**, 195467 (2011).
[10] B. Shin and M. J. Aziz, Phys. Rev. B **76**, 085431 (2007).
[11] M. Schmid, C. Lenauer, A. Buchsbaum, F. Wimmer, G. Rauchbauer, P. Scheiber, G. Betz, and P. Varga, Phys. Rev. Lett. **103**, 076101 (2009).
[12] D. Adamovic, V. Chirita, E. P. Munger, L. Hultman, and J. E. Greene, Phys. Rev. B **76**, 115418 (2007).
[13] J. Tersoff, A. W. Denier van der Gon, and R. M. Tromp, Phys. Rev. Lett. **72**, 266 (1994).
[14] G. Eres, J. Z. Tischler, M. Yoon, B. C. Larson, C. M. Rouleau, D. H. Lowndes, and P. Zschack, Appl. Phys. Lett. **80**, 3379 (2002).
[15] J. Z. Tischler, G. Eres, B. C. Larson, C. M. Rouleau, P. Zschack, and D. H. Lowndes, Phys. Rev. Lett. **96**, 226104 (2006).
[16] E. Vasco and J. L. Sacedon, Phys. Rev. Lett. **98**, 036104 (2007).
[17] J. R. Morales-Cifuentes, T. L. Einstein, and A. Pimpinelli, Phys. Rev. Lett. **113**, 246101 (2014).
[18] B. Hinnemann, H. Hinrichsen, and D. E. Wolf, Phys. Rev. E **67**, 011602 (2003).
[19] See Supplemental Material at http://link.aps.org/supplemental/10.1103/PhysRevLett.117.206102 for additional details on the film growth, experimental measurements, and data analysis, which contains Refs. [20,21].
[20] J. Z. Tischler, G. Eres, D. H. Lowndes, B. C. Larson, M. Yoon, T.-C. Cheng, and P. Zschack, in *Proceedings of the 11th U.S. National Synchrotron Radiation Instrumentation Conference (SRI99)*, edited by P. Pienetta, J. Arthur, and S. Brennan (AIP, New York, 2000), p. 151.
[21] K. W. Evans-Lutterodt and M. T. Tang, J. Appl. Crystallogr. **28**, 318 (1995).
[22] T. Vicsek and F. Family, Phys. Rev. Lett. **52**, 1669 (1984).
[23] D. Kandel, Phys. Rev. Lett. **78**, 499 (1997).
[24] A. Lo and R. T. Skodje, J. Chem. Phys. **112**, 1966 (2000).
[25] N. C. Bartelt, W. Theis, and R. M. Tromp, Phys. Rev. B **54**, 11741 (1996).
[26] M. Petersen, A. Zangwill, and C. Ratsch, Surf. Sci. **536**, 55 (2003).
[27] F. Hausser and A. Voigt, Phys. Rev. B **72**, 035437 (2005).
[28] J. A. Venables and H. Brune, Phys. Rev. B **66**, 195404 (2002).